Supporting Information 2

Examples of TEM results on Ag@Au nanoparticles

Daniel Llamosa Pérez, Manuel Ruano Díaz, Lidia Martínez, Alvaro Mayoral, Elisa Roman, Mar García-Hernández and Yves Huttel.

TEM measurements have been performed on nanoparticles deposited on ultrathin Carbon (< 3 nm) on carbon holey support films supported on Cu TEM grids. Representative TEM images are displayed in Figure S2.1.

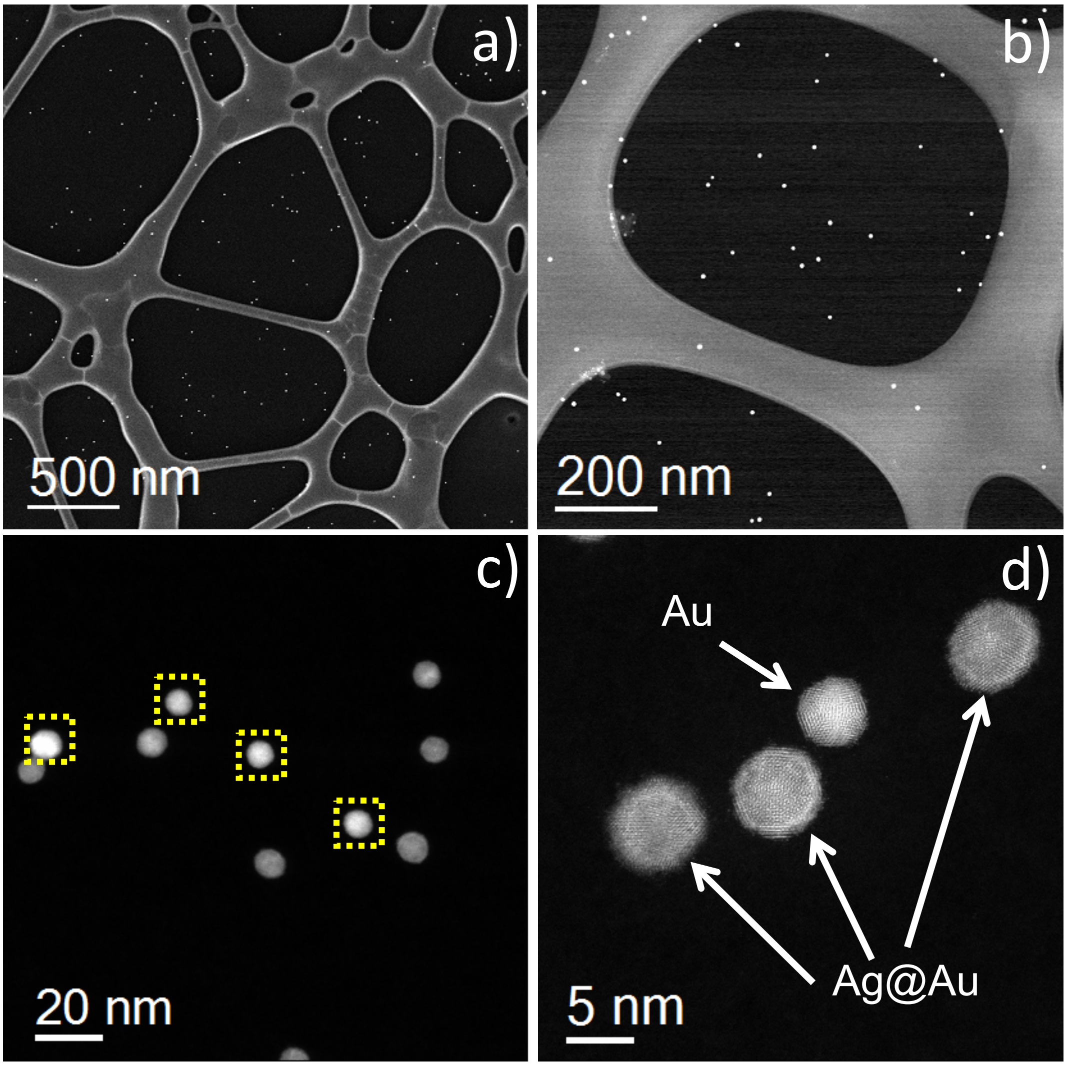

Figure S2.1 Cs-corrected STEM-HAADF images of NPs Ag@Au recorded at different magnifications.

In figure S2.1 a) and b) the lacey structure of the carbon support is clearly observed as well as the homogeneous nanoparticle distribution over the whole surface. The deposition time was 15 seconds and the deposition rate is approximately 2 NPs/$\mu m^2 s$. Such relatively low deposition rate is well suited for TEM grid deposition, but it can be increased several orders by changing the working parameters of the MICS. In figure S2.1 c) we have highlighted the pure Au nanoparticles by yellow squares. The pure Au nanoparticles can be distinguished from Ag@Au nanoparticles thanks to their higher intensity resulting from their higher density of electrons. High-resolution TEM inspection of pure Au and Ag@Au nanoparticles have confirmed that the nanoparticles could be recognized with modest magnification images as shown in the figure S2.1 c). At higher magnification, as displayed in figure S2.1 d) the distinction of pure Au NPs and Ag@Au NPs is even more straightforward since the bright shells of Au surrounding the Ag cores are distinguishable. Note that the size of pure Au NPs differs from the size of Ag@Au NPs as could be expected. Such size evolution as a function of NPs type allows the possibility to mass select the NPs using a quadrupole mass filter.

Depending on the working parameters applied to each of the magnetrons (argon flux, position in the aggregation zone and applied power), different types and concentrations of nanoparticles were observed. The best case, 50% of the nanoparticles were Ag@Au as expected while the other nanoparticles were pure Au NPs (39%) and Janus type NPs (11%). We found that the proportions of nanoparticles with different structures were very dependent on the working parameters. As an example, we display in figure S2.2a, a high magnification image were the order of 16% of the nanoparticles were agglomerated and in figure S2.2b were 30% of nanoparticles displayed a Janus type structure. These different types of nanoparticles are obtained by modifying the working parameters of the MICS. A detailed study on the influence of the working parameters on the generation of different types of nanoparticles will be presented in a further contribution.

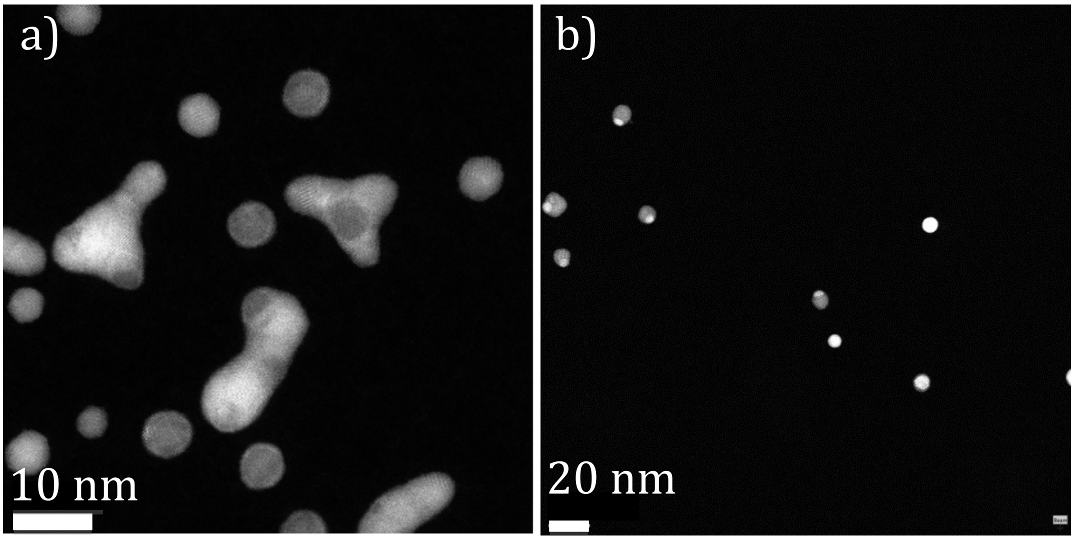

Figure S2.2. a) Example of agglomerated and b) Janus type nanoparticles.